Short communication

Iron complexes of [2+2] and [6+6] Schiff-base macrocycles derived from 2,2′-oxydianiline and their applications

Kuiyuan Wang [a], Kai Chen [b], Jiajun Cai [c], Carl Redshaw [a,*]

[a] Department of Chemistry, University of Hull, Hull HU6 7RX, UK
[b] Collaborative Innovation Center of Atmospheric Environment and Equipment Technology, Jiangsu Key Laboratory of Atmospheric Environment Monitoring and Pollution Control, School of Environmental Science and Engineering, Nanjing University of Information Science & Technology, Nanjing 210044, PR China
[c] MIIT Key Laboratory of Critical Materials Technology for New Energy Conversion and Storage School of Chemistry and Chemical Engineering State Key Lab of Urban Water Resource and Environment, Harbin Institute of Technology, Harbin 150001, PR China

ARTICLE INFO

ABSTRACT

Reaction of [2+2] and [6+6] Schiff-base macrocycles with $FeBr_2$ are reported, together with preliminary studies of the applications of the iron-containing products. In particular, we have investigated peroxidase-like activity and determination of H_2O_2, as well as their ability to act as catalysts for ring opening polymerization of cyclic esters.

1. Introduction

Macrocycles have attracted attention for decades, and their coordination chemistry is of particular interest given the possible simultaneous coordination of multiple metals centres and beneficial cooperative effects. We have investigated the coordination chemistry of [2+2] Schiff-base macrocycles derived from chelating anilines $\{2,2′-(X)(C_6H_4NH_2)_2\}$ $(X = CH_2CH_2, O)$ and diformylphenols $[1,3-(CHO)_2-5-X'-C_6H_3OH-2]$ $(X' = Me, tBu, Cl)$ [1–4]. Macrocycles which bear both phenoxide and accessible nitrogen groups are of biological interest [5–7], and their complexes have been employed as enzyme mimics [8–14]. Literature on [6+6] macrocycles and complexes thereof are scant [15–18]. The low toxicity associated with Fe(III), together with low cost of iron precursors, makes such systems attractive.

Herein, we explore iron chemistry of [2+2] macrocycles and a new [6+6] macrocycle (Charts S1 and S2). The syntheses of these macrocycles are solvent dependent, requiring refluxing methanol ([2+2]) or refluxing toluene ([6+6]). Initial studies on their peroxidase-like activity (and H_2O_2 determination), and use as catalysts for ROP of cyclic esters is reported.

2. Results and discussion

2.1. Synthesis and molecular structures

L^1H_2 $\{[2-(OH)-5-(Me)-C_6H_2-1,3-(CH)_2][O(2-C_6H_4N)_2]\}_2$ reacts with $FeBr_2$ (2.1 equivalents) in refluxing toluene resulting in the Fe(III) salt $[L^1H_2FeBr_2]_2[FeBr_3OFeBr_3]\cdot7MeCN$ (**1**·7MeCN). The formation of Fe (III) is likely due to adventitious oxygen, and appears to promote salt formation (see **3**). Views of the molecular structure are shown in Figs. S1/S2; bond lengths and angles in Table S1. In the cation, the iron centre is distorted octahedral and bound in *N,O,N,O*-fashion by the macrocycle; two *cis*-bromides complete the coordination sphere.

Similar reaction of L^1H_2, but in the presence of Et_3N, resulted in the Fe(II) complex $[Fe_2Br_2L^1]_2\cdot3MeCN$ (**2**·3MeCN) (Figs. S3/S4). The structure contains a distorted trigonal bipyramidal Fe1 ($\tau = 0.55$) and a distorted square pyramidal Fe2 ($\tau = 0.42$) [19].

L^1H_2 is available via a double condensation reaction in refluxing methanol [20], however, on changing to toluene (higher reflux temperature), the product is the [6+6] macrocycle L^2H_6, characterized by FT-IR, elementary analysis and ESI-MS ($^m/_z = 1972$ $([M + 3H]^+)$.

L^2H_6 $\{[2-(OH)-5-(Me)-C_6H_2-1,3-(CH)_2][O(2-C_6H_4N)_2]\}_6$ (L^2H_6) reacts with $FeBr_2$ (4.1 equivalents) affording $[Fe_2(L^2H_2)][FeBr_3OFeBr_3]\cdot4MeCN$ (**3**·4MeCN) (Figs. 1, S5); bond lengths/angles in Table S1. The structure is comprised of a dinuclear Fe(III) cation, an $[FeBr_3OFeBr_3]$ anion and four MeCN molecules. Each distorted octahedral iron centre

in the cation is bound by three phenoxide oxygens and three imine nitrogens. Fe—O bonds (e.g. for Fe1, 1.886(4)–1.974(4) Å) and Fe—N bonds (e.g. for Fe1, 2.157(4)–2.185(4) Å) compare favorably with those reported for iron(III) complexes bearing related macrocycles, e.g. [Fe $(L^3)(L^3H)]\cdot3MeCN$ $(L^3H_2 = \{[2-(OH)-5-(tBu)-C_6H_2-1,3-(CH)_2][CH_2CH_2(2-C_6H_4N)_2]\}_2$ [21]. There are noteworthy intermolecular interactions including C—H···π, Br–H and anion···π interactions (Fig. S6), connecting two neighboring macrocycles, with C-H···π interactions at *ca.* 3.455 Å and C-H-imine interactions *ca.* 3.667 Å. Br-H (2.807–3.309 Å) and anion···π interactions (3.475 Å) exist between anion and macrocycle.

The morphology of **1**–**3** was analyzed by SEM (Figs. S7-S9) and micrographs exhibiting nanorod-like morphology are observed. That for **2** reveals homogeneous "wing" shapes composed of needle-like crystals.

2.2. Ring opening polymerization of cyclic esters

The potential of **1**–**3** to act as catalysts for ring-opening polymerization (ROP) was evaluated. A variety of conditions (differing ratios of [monomer]:[Cat]:[BnOH], temperatures and times) were used in the attempted ROP of ε-caprolactone, δ-valerolactone and *r*-lactide, however there was no sign of oligomeric/polymeric products. Byers et al. have reported that iron-based ROP catalysts are sensitive to metal oxidation state and associated electron density [22,23]. Activity was disfavored by the presence of cationic ferric centres, as observed for **1** and **3** herein. Given the inactivity associated with **2**, we cannot rule out the formation of similar ferric salt formation under the employed catalytic conditions.

2.3. Peroxidase-like activity

The peroxidase-like activity of **1**–**3** was tested via oxidation of 3,3′,5,5′- tetramethylbenzidine (TMB) in the presence of H_2O_2.

TMB can be oxidized by H_2O_2 in the presence of **1**–**3** forming oxTMB, which exhibits a blue color (absorption at 652 nm); no color changes were found when using only L^1H_2 or L^2H_6. TMB oxidation only occurs in the Fe-TMB-H_2O_2 system, whereas no oxidation is observed in either the Fe-TMB or TMB-H_2O_2 systems (Fig. 2). With optimum pH = 4, the maximum absorbance was obtained at 45 °C (**1** and **2**) or 50 °C (**3**) (Fig. S10). Steady-state kinetic measurements were conducted and Lineweaver–Burk plots for **1**–**3** are shown in Figs. S11–S13; the double reciprocal plot is near linear [12]. For calculated V_{max} (maximal reaction velocity) and K_m values for **1**–**3** towards H_2O_2 and TMB, see Table S2. The V_{max} values of these complexes are higher than for HRP and Fe_3O_4, suggesting they are good peroxidase-like mimetics. Leaching experiments revealed no activity, ruling out Fenton-type behavior from free Fe^{2+} [24,25].

The possible electron transfer process of the Fe-TMB-H_2O_2 systems was investigated by cyclic voltammograms. Reduction currents of H_2O_2 were observed using a Fe modified glassy carbon electrode as working
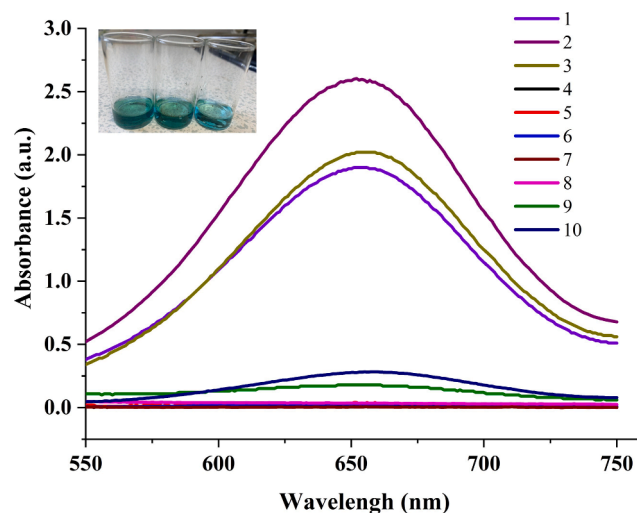

Fig. 2. Absorbance spectra of oxTMB: 1) **1** + TMB + H_2O_2; 2) **2** + TMB + H_2O_2; 3) **3** + TMB + H_2O_2; 4) **1** leaching solution + TMB + H_2O_2; 5) **2** leaching solution + TMB + H_2O_2; 6) **3** leaching solution + TMB + H_2O_2; 7) TMB + H_2O_2; 8) **2** leaching solution + TMB; 9) **2** + TMB; 10) **3** + TMB; Insert: color change of samples (left to right: using **1**, **2** and **3**, respectively).

electrode. It was deduced that **1**–**3** accelerate the electron transfer process between TMB and H_2O_2 (Fig. 3) [26,27]. The system employing **1** or **3** exhibits best reduction current, assigned to the presence of Fe(III) centres (*versus* Fe(II) in **2**).

The colorimetric method for H_2O_2 sensing was based on the amount of blue oxTMB and is proportional to [H_2O_2]. Two linear ranges were obtained (Fig. S14), 0.5–5 mM, and 6–10 mM, with detection limit 0.05 mM. The selectivity was tested with 5 mM H_2O_2 and the concentration of interferences was 4-fold that of H_2O_2 (Fig. S15). Results indicated an efficient method even in the presence of potentially competing contaminants. A comparison of the linear range and detection limit of different H_2O_2 sensors using peroxidase mimetics is shown in Table S3; this method possesses a comparatively wide linear range and low LOD.

3. Conclusion

[2+2] or [6+6] Schiff-base macrocycles have been complexed with Fe, and used as horseradish peroxidase mimetics. At pH 4.0, they exhibit highest absorbance at 652 nm, whilst 45 °C (**1, 2**) and 50 °C (**3**) are preferred temperatures. From kinetic studies, Michaelis–Menten type kinetics is exhibited and the process of electron transfer between TMB and H_2O_2 was found to be accelerated by the Schiff-base iron complex. Based on peroxidase mimic activity, a colorimetric determination method for H_2O_2 using **3** was established, with good selectivity with linear ranges (0.5–5 mM and 6–10 mM) and low detection limit (0.05
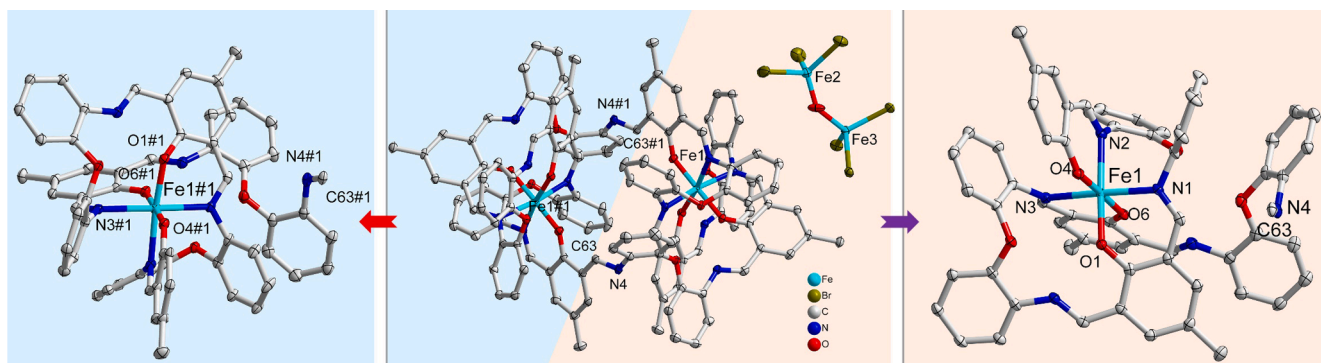

Fig. 1. Molecular structure of [$Fe_2(L^2H_2)$][$FeBr_3OFeBr_3$]·4MeCN (**3**·4MeCN), with ellipsoids at 30% probability level.
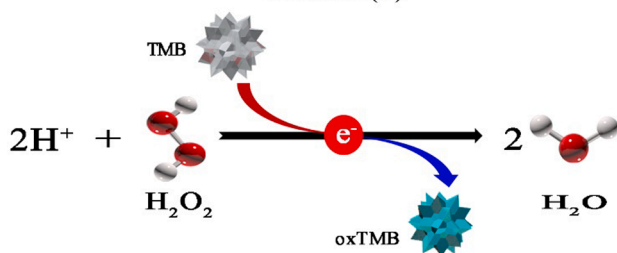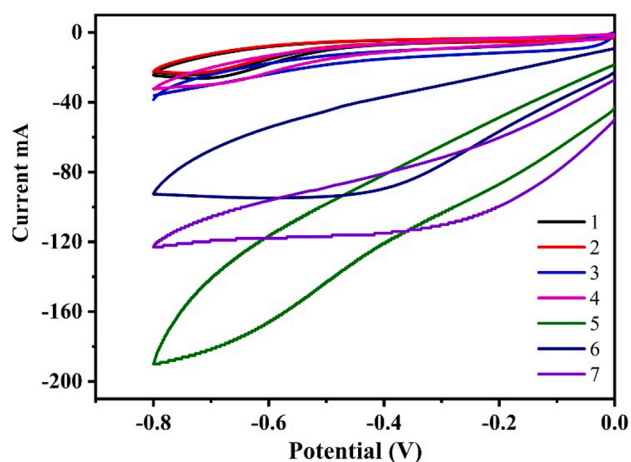
Fig. 3. Cyclic Voltammograms (pH = 4.0) using **1**–**3** 1) buffer; 2) **1** modified GCE + buffer; 3) **2** modified GCE + buffer; 4) **3** modified GCE + buffer; 5) **1** modified GCE + buffer + 20 mM H_2O_2; 6) **2** modified GCE + buffer; 7) **3** modified GCE + buffer.

mM). Such iron complexes are ineffective as catalysts for ROP of cyclic esters.

CRediT authorship contribution statement

Kuiyuan Wang: Investigation. **Kai Chen:** Investigation. **Jiajun Cai:** Investigation. **Carl Redshaw:** Funding acquisition, Supervision, Writing – review & editing.

Declaration of Competing Interest

The authors declare that they have no known competing financial interests or personal relationships that could have appeared to influence the work reported in this paper.

Acknowledgements

Appendix A. Supplementary material

Supporting information includes: 1) Experimental; 2) Views of structures; 3) Effects of pH and temperature on peroxidase-like activity of the complexes; 4) Steady state kinetic assays of **1** – **3**; 5) Crystallographic data for **1** – **3** (Table S4). Supplementary data to this article can be found online at https://doi.org/10.1016/j.inoche.2022.109376.

References

[1] A. Arbaoui, C. Redshaw, D.L. Hughes, Chem. Commun. 39 (2008) 4717–4719.
[2] W. Yang, K.Q. Zhao, T.J. Prior, D.L. Hughes, A. Arbaoui, T. Bian, M.R.J. Elsegood, C. Redshaw, Dalton Trans. 45 (2016) (2005) 11990–11991.
[3] C. Redshaw, Catalysts 7 (2017) 165.
[4] K. Wang, T.J. Prior, C. Redshaw, Chem. Commun. 55 (2019) 11279–11282.
[5] S. Ali, V. Singh, P. Jain, V. Tripathi, J. Saud. Chem. Soc. 23 (2019) 52.
[6] A.G.B. Dileepan, T.D. Prakash, A.G. Kumar, P.S. Rajam, V.V. Dhayabaran, R. Rajaram, J. Photochem. Photobiol. B: Biol. 183 (2018) 191.
[7] P.M. Reddy, A.V.S.S. Prasad, K. Shanker, V. Ravinder, Spectrochim. Acta A 68 (2007) 1000.
[8] V. Staveren, C.J. Fenton, D.E. Reinhoudt, D.N. Van Eerden, J.S. Harkema, J. Am. Chem. Soc. 109 (1987) 3456–3458.
[9] P. Zucca, G. Mocci, A. Rescigno, E. Sanjust, J. Mol. Catal. A: Chem. 278 (2007) 220–227.
[10] T.T. Liu, J. Tian, L. Cui, Q.Y. Liu, L.L. Wu, X.M. Zhang, Colloids Surf. B 178 (2019) 137.
[11] S. Bhakta, A. Nayek, B. Roy, A. Dey, Inorg. Chem. 58 (2019) 2954–2964.
[12] Y. Hitomi, K. Hiramatsu, K. Arakawa, T. Takeyasu, M. Hata, M. Kodera, Dalton Trans. 42 (2013) 12878–12882.
[13] G. Kumar, S. Devi, R. Johari, D. Kumar, Eur. J. Med. Chem. 52 (2012) 269–274.
[14] A.D. Ryabov, R.C. Camacho, O.S. Díaz, M.A. Denardo, Anindya Ghosh, T.J. Ronan Le Lagadec, T.J. Collins, Anal. Chem. 84 (2012) 9096–9100.
[15] J. Hui, M. MacLachlan, Chem. Commun. 23 (2006) 2480.
[16] S. Srimurugan, P. Suresh, H.N. Pati, J. Inclusion Phenom. Macrocyclic Chem. 59 (2007) 383–388.
[17] J. Gregoliński, K. Ślepokura, T. Paćkowski, J. Lisowski, Org. Lett. 16 (2014) 4372.
[18] D.S. Nesterov, O.V. Nesterova, M.F.C. Guedes da Silva, A.J.L. Pombeiro, Catal, Sci. Technol. 5 (2015) 1801–1812.
[19] A.W. Addison, T.N. Rao, J. Reedijk, G.C. van Rijn, J. Verschoor, J. Chem. Soc. Dalton Trans. 7 (1984) 1349–1356.
[20] K. Chen, Z.Y. Hua, R. Li, Y.Y. Peng, Q.Z. Zhu, J.L. Zhao, C. Redshaw, CrystEngComm 23 (2021) 465–481.
[21] K. Wang, T.J. Prior, D.L. Hughes, A. Arbaoui, C. Redshaw, Dalton Trans. 50 (2021) 8057–8069.
[22] A.B. Biernesser, B. Li, J.A. Byers, J. Am. Chem. Soc. 135 (2013) 16553–16560.
[23] C.M. Manna, H.Z. Kaplan, B. Li, J.A. Byers, Polyhedron 84 (2014) 160–167.
[24] L. Rastogi, D. Karunasagar, R.B. Sashidhar, A. Giri, Sens. Actuators, B 240 (2017) 1182–1188.
[25] J. Guo, Y. Wang, M. Zhao, Talanta 182 (2018) 230–240.
[26] J. Mu, Y. Wang, M. Zhao, L. Zhang, Chem. Commun. 48 (2012) 2540–2542.
[27] J. Wang, Y.Y. Hu, Q. Zhou, L.Z. Hu, W.S. Fu, Y. Wang, ACS Appl. Mater. Interfaces 11 (2019) 44466–44473.